Hindawi
Mathematical Problems in Engineering
Volume 2020, Article ID 4214379, 18 pages
https://doi.org/10.1155/2020/4214379

Research Article

Collapse Risk Analysis of Deep Foundation Pits in Metro Stations Using a Fuzzy Bayesian Network and a Fuzzy AHP

Guohua Zhang,[1] Chengtang Wang,[1,2] Yuyong Jiao,[3] Hao Wang,[1] Weimin Qin,[1] Wu Chen,[1,2] and Guoqiang Zhong[4]

[1]*State Key Laboratory of Geomechanics and Geotechnical Engineering, Institute of Rock and Soil Mechanics, Chinese Academy of Sciences, Wuhan, Hubei 430071, China*
[2]*University of Chinese Academy of Sciences, Beijing 100049, China*
[3]*Faculty of Engineering, China University of Geosciences, Wuhan 430074, China*
[4]*Shandong Provincial Communication Planning and Design Institute, Jinan, Shandong 250031, China*

Correspondence should be addressed to Yuyong Jiao; yyjiao@cug.edu.cn

Received 14 December 2019; Revised 20 February 2020; Accepted 22 February 2020; Published 27 April 2020

Academic Editor: Daniela Addessi

Collapse risk analysis is of great significance for ensuring construction safety in foundation pits. This study proposes a comprehensive methodology for dynamic risk analysis of foundation pit collapse during construction based on a fuzzy Bayesian network (FBN) and a fuzzy analytical hierarchy process (FAHP). Firstly, the potential risk factors contributing to foundation pit collapse are identified based on the results of statistical analysis of foundation pit collapse cases, expert inquiry, and fault tree analysis. Then, a FAHP and improved expert elicitation considering a confidence index are adopted to elicit the probability parameters of the BN. On this basis, quantitative risk reasoning and sensitivity analysis of foundation pit collapse are achieved by means of fuzzy Bayesian inference. Finally, an actual deep foundation pit in a metro station was used to illustrate a specific application of this approach, and the results were in accordance with the field observations and numerical simulation results. The proposed approach can provide effective decision-making support for planners and engineers, which is vital to the prevention and control of the occurrence of the foundation pit collapse accidents.

1. Introduction

With the rapid development of urbanization around the world, metros have become a promising solution for relieving overground traffic in congested urban areas. However, metro construction is exposed to large potential risks due to various potential risk events in an uncertain environment. Therefore, the number of accidents is increasing in metro engineering, especially in developing countries such as China. For example, on November 15, 2008, 21 people were killed in a collapse caused by the diaphragm wall failures in the Xianghu Station of Hangzhou Metro Line 1 [1]. Additionally, an accident that occurred in the Haizhu Square Station of Guangzhou Metro Line 2 caused five people to be trapped, and nearby buildings were cracked as a result of a diaphragm wall collapse [2]. As we can see, the frequent occurrence of foundation pit collapse accidents in metro construction has led to serious consequences and aroused the attention of all parties, including the public [3].

In recent decades, various risk assessment approaches developed based on probabilistic risk analysis (PRA) have been widely used in construction projects to avoid financial losses and personnel casualties. For example, these approaches include Monte Carlo simulations (MCS) [4, 5], event tree analysis (ETA) [6, 7], fault tree analysis (FTA) [8, 9], and decision trees (DT) [10]. The above-mentioned methods have played a vital role in improving the risk management and control ability of large construction projects [11, 12]; however, in many circumstances, these methods are incapable of coping well with uncertainties and giving satisfactory results on account of incompleteness or shortage of data [13]. Furthermore, it is often difficult or

sometimes even impossible to obtain statistical data for PRA modeling, and this approach often relies on expert knowledge and experience. In recent years, the fuzzy reasoning methods [14–17] and fuzzy hybrid methods [18–20] have been developed based on fuzzy set theory (FST) [21] to overcome the limitations of PRA methods. Although the fuzzy reasoning and fuzzy hybrid methods can solve engineering problems under uncertainty, these methods suffer from limitations in conducting inference inversely and dynamic risk analysis. Feed-forward-like approximate reasoning approaches are strictly one way; that is, when a model is given a set of inputs, it can predict the output, but not vice versa [22–24]. This may have limitations on the flexibility of a safety analysis and assessment method that focuses on exploring causal relationships among risk factors. Furthermore, the aforementioned methods have a limitation in effectively achieving dynamic risk analysis and cannot achieve real-time safety control. When related parameters such as hydrological and geological parameters are changed, the above-mentioned approaches cannot accurately handle the updated features of dynamic process in project construction. Therefore, effective real-time safety measures cannot be implemented with a change in environment [25].

Recently, Bayesian networks (BNs) have been developed to model the complexity of man-machine systems [26] and are widely used in many fields to perform uncertain knowledge representation and probabilistic reasoning because of the ability to represent multistate variables, dependencies among variables, and update probabilities [25, 27, 28]. Sousa and Einstein [29] presented a BN-based risk analysis approach for decision support in tunnel construction. Liang et al. [30] used BNs to conduct risk assessment of debris flow hazards. Khakzad et al. [31] performed a quantitative risk assessment of drilling operations based on a bow-tie and BN method. Zhou et al. [32] conducted quantitative risk analysis in foundation pit construction project based on the BN and field data.

Although BN has many advantages, it also has the limitation of using a probability measure to assess uncertainty. Traditional BNs can achieve quantitative risk analysis if exact information is sufficient and available [33], which is nearly impossible owing to lack of detailed data and incomplete knowledge, especially for construction projects [34, 35]. As mentioned earlier, FST provides a powerful tool to deal with uncertainties and ambiguities associated with engineering problems [36]. Therefore, the combination of fuzzy logical and BN theory may provide an alternative means to carry out risk assessment under an uncertainty environment [37]. A fuzzy BN-based safety risk analysis model was proposed for risk assessment of tunnel-induced pipeline damage by Zhang et al. [37]. Wang and Chen [38] introduced a systematic risk assessment method for metro construction using a fuzzy comprehensive BN. Similarly, Sun et al. [39] utilized a multistate fuzzy Bayesian network (FBN) to conduct risk analysis of tunnel collapse. Compared with traditional BN, FBN seems more flexible and interpretable [22]. Moreover, conventional BN can only handle precise probabilities, which in most cases are difficult to estimate, especially for large and complex projects. As FBN incorporates the advantages of both FST and BN, it can deal more effectively with uncertainty of risk data and describe the dependent and complex relationships between risk events [23, 40, 41]. Nevertheless, the elicitation of prior probabilities and conditional probability tables (CPTs) under data shortage or incompleteness is one of the key challenges to be solved.

In the above-mentioned studies, the probability parameters are usually determined via expert elicitation to overcome the incompleteness or lack of data, and linguistic expressions and integral value methods are usually adopted to quantify prior probabilities. However, the involvement of human judgement inevitably brings subjectivity and vagueness and thus causes the subsequent probability analysis to be unreliable and untrustworthy. In addition, the elicitation of large number of probability parameters of the BN not only puts great workload on the experts but also poses challenges to the quality or consistency of the elicited result [42]. Additionally, most of the existing researches focus mainly on risk analysis of tunnel construction, whereas few cases of foundation pit construction are reported. However, the foundation pit construction may face more potential risks than tunnel construction due to its more complex surroundings.

In construction practice, various risk factors including internal (geological, hydrological, etc.) and external ones (construction, organization, etc.) are able to lead to foundation pit collapse. Thus, a systematic and integrated method is required to carry out collapse risk analysis of foundation pit in construction, and this is of great significance for ensuring construction safety. A comprehensive methodology for quantitative risk analysis is presented in this study to compensate for the shortcomings of existing models. Firstly, the potential risk factors that contribute to foundation pit collapse are identified via FTA. Thereafter, a fault tree (FT) model is transformed into a corresponding BN model to conduct quantitative risk reasoning. Then, the FAHP technique is adopted in this study to determine the prior probabilities and CPTs of nodes in BN, as it can overcome subjectivity and ambiguity issues and is an effective approach for handling uncertainty associated with expert evaluations. Moreover, a decomposition method is used to eliminate the number of comparisons as well as reducing possibility of inconsistency. Finally, the sensitivity performance measure is applied for sensitivity analysis to determine the critical risk factors for foundation pit collapse.

The remainder of this paper is structured as follows. Section 2 presents the developed methodology for risk analysis of foundation pit collapse based on a FBN and a FAHP. A case study of an actual deep foundation pit in Qianhu Avenue Station is described in Section 3. Section 4 discusses issues to be further studied, and conclusions are given in Section 5.

2. The Developed Methodology

To decrease the occurrence probability of collapse risk and ensure safe construction of foundation pit, a comprehensive methodology for risk analysis of foundation pit collapse is

developed based on a FBN and a FAHP. The following five steps are included in the proposed approach: (1) risk identification and FT construction based on expert knowledge and collected information; (2) FBN model establishment; (3) prior probability elicitation of the root nodes based on the FAHP and improved expert elicitation; (4) CPT elicitation of the intermediate nodes and leaf node using the FAHP, decomposition method, and improved expert elicitation; and (5) FBN-based risk reasoning and sensitivity analysis. The overall procedure for risk analysis of foundation pit collapse based on a FBN and a FAHP is shown in Figure 1.

2.1. Fuzzy Bayesian Network. In traditional BN, the failure probability of nodes is usually treated as a precise value, but insufficient data often makes it difficult or even impossible to obtain crisp probabilities, especially for construction projects [25]. In construction engineering fields, the occurrence probabilities of basic events are usually more imprecise and vague due to deviation of measured values, construction operation errors, engineering experience, and other factors. As FST aims to cope with uncertainties caused by imprecision and fuzziness, a BN model integrated with FST is developed, and this combination is referred to as a FBN. Moreover, many studies have shown that a FBN not only can produce similar results with the same model and similar input data but also is more flexible and interpretable than a traditional BN and is the inheritance and development of a traditional BN [22, 23].

2.2. Risk Identification and FT Construction. Risk identification involves carrying out risk mechanism analysis for accidents and documenting their characteristics. In this paper, we analyze the risk mechanism of foundation pit collapse from internal factors (hydrogeological conditions) and external factors (design, construction, management factors, etc.) and reveal the causal relationships between risk factors via FTA. In addition, domain experts are also invited to query risk factors according to the construction site conditions and collected material (the literature, construction standards, and technical manuals). Then, the final FT model of foundation pit collapse can be built by combining the results of FTA and expert inquiry.

2.3. Mapping the FT into a Bayesian Network. BN construction is usually complex and is the "bottleneck" of its further application in safety risk analysis. The method of BN construction based on FT transformation is considered an effective approach to solve the above problem. Hence, BN construction based on the method of mapping the FT into a BN is adopted in the present study. Mapping from FT into the BN is based on graphical and numerical functions, and the specific mapping procedure is shown in Figure 2 [27]. In graphical mapping, the primary events, intermediate events, and the top event of the FT are directly transformed into root nodes, intermediate nodes, and the leaf node in an equivalent BN, respectively [28]. Overlapping nodes are merged into one [40]. In numerical mapping, the occurrence probabilities of the primary events in the FT are assigned to the relevant root nodes of the BN as a priori probabilities. CPTs are developed based on the Boolean gates of the FT.

2.4. Prior Probabilities and CPT Establishment. Generally, the prior probabilities and CPTs of BN can be obtained based on a shrinkage approach [43] or hill climbing algorithms [44] if sufficient available data are collected. However, it is very difficult to present enough available data in engineering practice for BN model construction and parameterization due to the rare occurrence of foundation pit collapse and the limits of various learning algorithms. Therefore, experts' domain knowledge and experience remain important sources for BN modeling, and the establishment of probability parameters of BN still relies on expert elicitation. However, the involvement of human judgement inevitably brings subjectivity and vagueness. Thus, in this study, a FAHP was employed to handle the uncertainty and ambiguity of criteria and the judgement process. Moreover, an improved expert elicitation method based on a confidence index was used to guarantee survey data reliability, which takes both objectivity and subjectivity into account. An expert's judgement ability is determined according to his/her designation, educational level, and service time. The judgement ability level represented by ξ is determined based on the four indicators including expert's designation, educational level, service time, and age, and the corresponding expert judgement ability level is computed using a FAHP method. The system of expert information is illustrated in Figure 3. The expert profiles and judgement ability level calculated via the FAHP are shown in Table 1. The higher the value of ξ is, the more reliable the expert judgement will be.

In addition, the subjective reliability level represented by ψ is utilized to measure the reliability of experts' judgements on their own and is also divided into five levels, represented by "0.6, 0.7, 0.8, 0.9, and 1.0." The higher the value of ψ is, the more certain the judgement will be. When N experts are involved, the confidence index of the kth expert, indicated by θ_k, can be calculated by (1). If the expert cannot make a judgement about his/her subjective reliability level or give a subjective reliability level ψ less than 0.6, the data will not be adopted.

$$\theta_k = \xi_k \times \psi_k. \tag{1}$$

The processes of combining FAHP, decomposition method, and improved expert elicitation to establish prior probabilities and CPTs of BN are shown in the following steps.

2.4.1. Generation of Root Nodes' Prior Probabilities. In such circumstances, assume that there are n states ($S_1, S_2, \ldots, S_n$) of a node N, and the probability of N at state S_i is denoted by $P(S_i)$. Generally speaking, $P(S_i)$ is usually elicited by experts according to their experience, and it may be feasible while the number of nodes' states is not large. However, estimating probabilities to all states at a time is difficult when the number of states is large and the BN model structure is

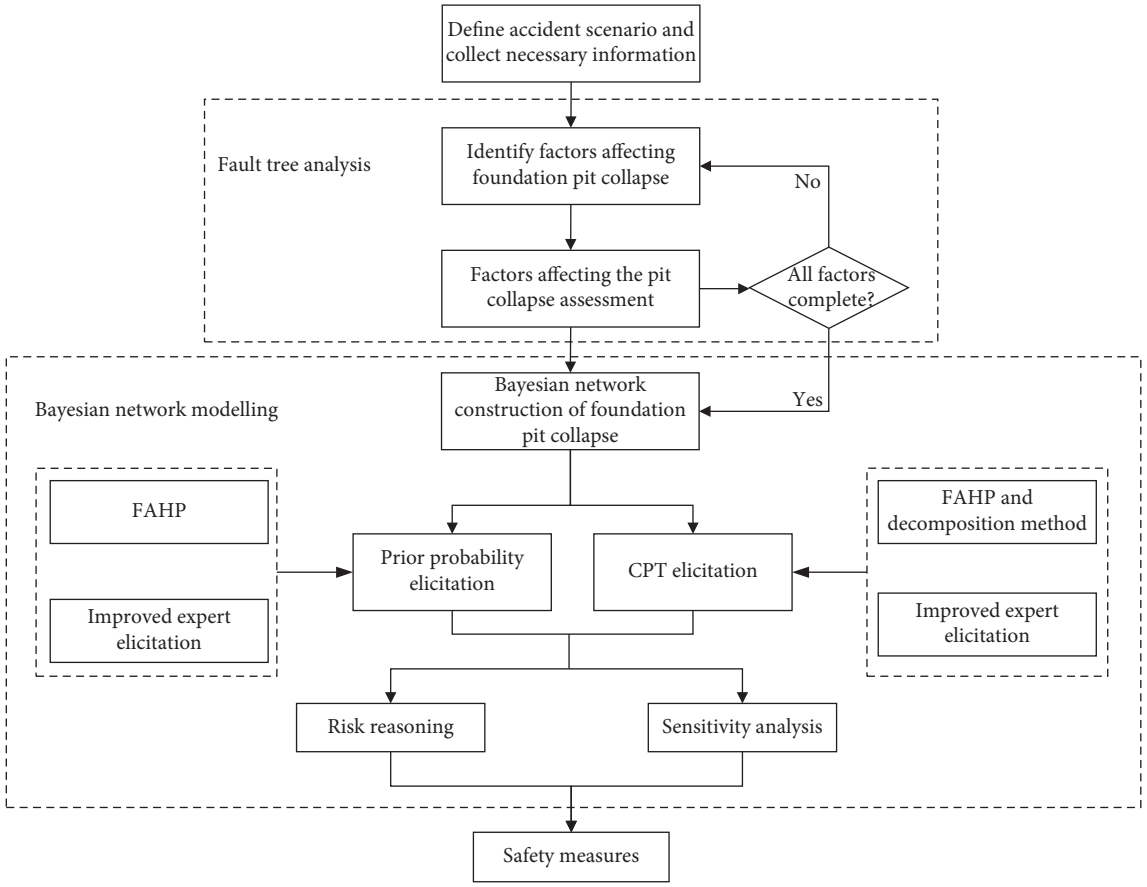

Figure 1: The overall procedure for risk analysis of foundation pit collapse based on a FBN and FAHP.

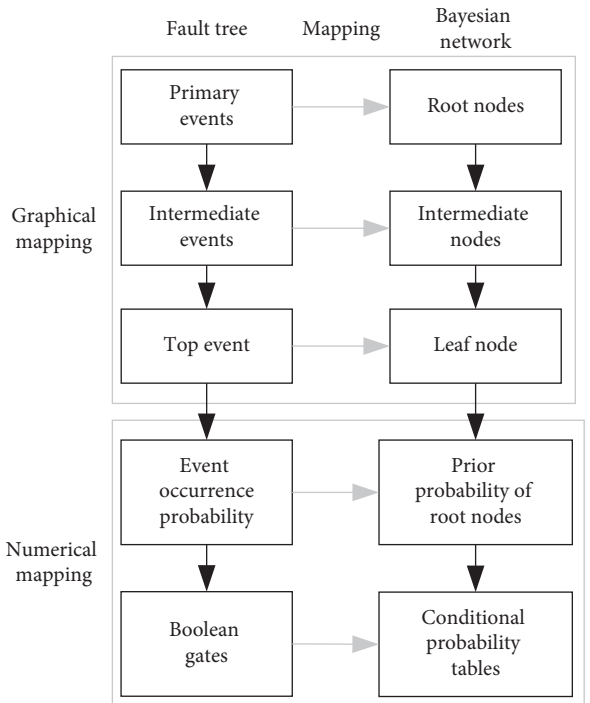

Figure 2: Mapping procedure from a FT to a BN [28].

complex [45]. Moreover, it may inevitably bring uncertainty and bias during expert elicitation. As mentioned earlier, the fuzzy AHP, a decomposition method, and improved expert elicitation are adopted in this paper to elicit probability parameters of BN as follows.

Each expert individually implement a pairwise comparison according to Saaty's 1–9 scale [46], and $A^{(k)} = [a_{ij}^{(k)}]_{n\times n}$ represents the pairwise comparison matrix obtained from the kth expert. Furthermore, each expert should also give his/her subjectivity reliability level ψ_k towards his/her own judgements. Then, the fuzzy positive reciprocal matrix $\widetilde{A} = [\widetilde{a}_{ij}]_{n\times n}$ can be obtained by integrating M experts' grades using (2), where $\widetilde{a}_{ij}$ is a TFN with

$$\widetilde{a}_{ij} = \begin{cases} [1,1,1], & i = j, \\ \left[l_{ij}, m_{ij}, u_{ij}\right] = \left[\dfrac{1}{u_{ji}}, \dfrac{1}{m_{ji}}, \dfrac{1}{u_{ji}}\right], & i \neq j, \end{cases}$$

$$l_{ij} = \min_{1\le k\le M}\left\{a_{ij}^{(k)}\right\}, \tag{2}$$

$$m_{ij} = \sum_{k=1}^{M} \frac{\theta_k}{\sum_{k=1}^{M}\theta_k} a_{ij}^{(k)},$$

$$u_{ij} = \max_{1\le k\le M}\left\{a_{ij}^{(k)}\right\},$$

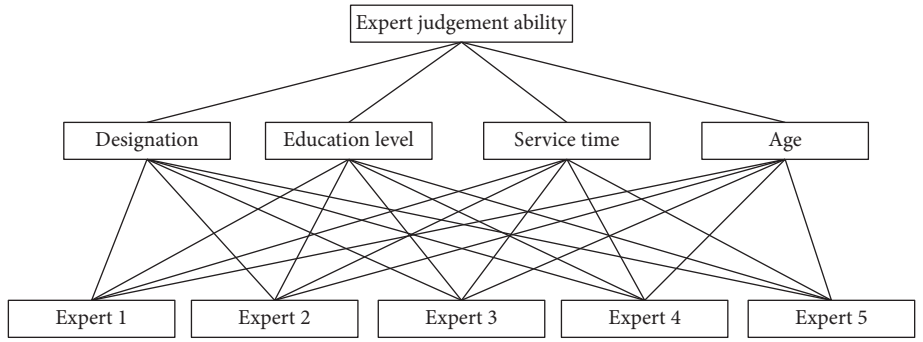

Figure 3: Fuzzy AHP index system of respective expert judgement ability.

Table 1: Experts' profile and related judgement ability level.

No.	Designation	Education level	Service time (year)	Age	Judgement ability level (ξ)
Expert 1	Professor	Doctoral	24	52	0.246
Expert 2	Associate professor	Doctoral	16	44	0.202
Expert 3	Senior engineer	Doctoral	18	46	0.221
Expert 4	Engineer	Masters	11	38	0.150
Expert 5	Senior engineer	Masters	14	40	0.181

where M is the number of experts, θ_k denotes the confidence index of the kth expert and can be obtained by (1), and $\theta_k / \sum_{k=1}^{M} \theta_k$ represents the degree of reliability regarding the judgement data of the kth expert.

In addition, the consistency of fuzzy matrix $\widetilde{A}$ should be tested before the calculation of weight [47]. A new judgement matrix $\widetilde{A}$ must be obtained again when the above test results are inconsistent until the consistency of matrix $\widetilde{A}$ is verified to be acceptable.

After the consistency test, the fuzzy weight matrix can be calculated by (3)–(5). First, the geometric means of the TFNs for the ith state of node N can be obtained as

$$g_i = \left(\prod_{j=1}^{k} a_{ij}\right)^{1/k} = \left[\left(\prod_{j=1}^{k} a_{ij}\right)^{1/k}, \left(\prod_{j=1}^{k} m_{ij}\right)^{1/k}, \left(\prod_{j=1}^{k} u_{ij}\right)^{1/k}\right], \quad i = 1, 2, \ldots, k. \tag{3}$$

By summing up the g_i values, we have

$$\sum_{i=1}^{k} g_i = \left[\sum_{i=1}^{k}\left(\prod_{j=1}^{k} l_{ij}\right)^{1/k}, \sum_{i=1}^{k}\left(\prod_{j=1}^{k} m_{ij}\right)^{1/k}, \sum_{i=1}^{k}\left(\prod_{j=1}^{k} u_{ij}\right)^{1/k}\right], \quad i = 1, 2, \ldots, k. \tag{4}$$

Then, the fuzzy weight $\widetilde{w}_i$ related to the prior probability of the ith state of node N can be computed as follows:

$$\widetilde{w}_i = \left(\widetilde{w}_i^l, \widetilde{w}_i^m, \widetilde{w}_i^u\right) = \frac{g_i}{\sum_{i=1}^{k} g_i} = \left[\left(\frac{\left(\prod_{j=1}^{k} l_{ij}\right)^{1/k}}{\sum_{i=1}^{k}\left(\prod_{j=1}^{k} u_{ij}\right)^{1/k}}\right), \left(\frac{\left(\prod_{j=1}^{k} m_{ij}\right)^{1/k}}{\sum_{i=1}^{k}\left(\prod_{j=1}^{k} m_{ij}\right)^{1/k}}\right), \left(\frac{\left(\prod_{j=1}^{k} u_{ij}\right)^{1/k}}{\sum_{i=1}^{k}\left(\prod_{j=1}^{k} m_{ij}\right)^{1/k}}\right)\right], \quad i = 1, 2, \ldots, k. \tag{5}$$

Since the fuzzy weight $\widetilde{w}_i$ obtained above is a fuzzy number, the "α-weighted valuation defuzzification technique" proposed by Detyniecki and Yager [48] is selected here to convert fuzzy results into crisp values. Defuzzification of a TFN $\widetilde{w} = (\widetilde{w}_i^l, \widetilde{w}_i^m, \widetilde{w}_i^u)$ is shown in

$$\mathrm{Val}\left(\widetilde{w}_i\right) = \frac{\int_0^1 \mathrm{Average}\left(F_\alpha\right) \times f_\alpha \mathrm{d}\alpha}{\int_0^1 f(\alpha)\mathrm{d}\alpha}, \tag{6}$$

where $\mathrm{Val}(\widetilde{w}_i)$ denotes the transformed exact value, $F_\alpha = (x \mid F(x) \geq \alpha)$ is the α-level set of F, $f(\alpha)$ represents the α-weighted valuation function, and $\mathrm{Average}(F_\alpha)$ is the average of the α-level set and can be obtained as follows:

$$\mathrm{Average}\left(F_\alpha\right) = \frac{u_\alpha + v_\alpha}{2}, \tag{7}$$

where u_α and v_α can be determined with the help of Figure 4. Generally, we set $f(\alpha) = 1$ and $\alpha = 0.5$, and then, we can obtain the value of $\mathrm{Val}(\widetilde{w}_i)$, as shown in (10).

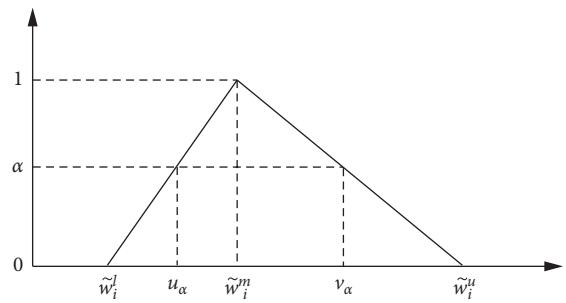

Figure 4: Membership function of a TFN $\tilde{w}_i$.

$$u_\alpha = \left(\tilde{w}_i^m - \tilde{w}_i^l\right) \times \alpha + \tilde{w}_i^l, \tag{8}$$

$$v_\alpha = \tilde{w}_i^u - \left(\tilde{w}_i^u - \tilde{w}_i^m\right) \times \alpha, \tag{9}$$

$$\begin{aligned} w_i = \mathrm{Val}\left(\tilde{w}_i\right) &= \frac{(1/2)\int_0^1 \left[\left(\tilde{w}_i^m - \tilde{w}_i^l\right) \times \alpha + \tilde{w}_i^l + \tilde{w}_i^u + \left(\tilde{w}_i^m - \tilde{w}_i^u\right) \times \alpha\right] \mathrm{d}\alpha}{\int_0^1 \mathrm{d}\alpha} \\ &= \frac{1}{2}\left(\tilde{w}_i^l + \tilde{w}_i^u + \frac{\tilde{w}_i^m - \tilde{w}_i^l}{2} + \frac{\tilde{w}_i^m - \tilde{w}_i^u}{2}\right) = \frac{\tilde{w}_i^l + 2\tilde{w}_i^m + \tilde{w}_i^u}{4}. \end{aligned} \tag{10}$$

Finally, $P(S_i)$ can be obtained via normalization of w_i as

$$P\left(S_i\right) = \omega_i = \frac{w_i}{\sum_{i=1}^n w_i}. \tag{11}$$

2.4.2. CPT Establishment for a Node with One Parent. Assuming that node N and its only parent M have n states (S_{N1}, S_{N2}, ..., S_{Nn}) and m states (S_{M1}, S_{M2}, ..., S_{Mm}), respectively, our aim is to derive the probabilities of each state of node N when the parent M is at state M_j, i.e., $P(S_{Ni} \mid S_{Mj})$ ($i = 1, 2, \ldots, n$; $j = 1, 2, \ldots, m$). We can judge which one (the states S_{Ni} and $S_{N\eta}$ ($\eta = 1, 2, \ldots, n$)) is more likely to occur when given the state of S_{Mj} by inquiring experts [45]. And each expert only needs to fill in the number represented by a_{ij} shown in Table 2. Thus, the corresponding comparison matrix is constructed as in the table.

Thus, $p(S_{Ni} \mid S_{Mj}) = w_{ij}$ can be obtained from the calculation of the above matrix, and the calculation procedure is the same as the generation of root nodes' prior probabilities. Since node M has m states, m matrices should be constructed to obtain all w_{ij} ($i = 1, 2, \ldots, n$; $j = 1, 2, \ldots, m$) values, which are the CPTs of the node N. Therefore, we can establish the CPTs for a single-parent node based on the above procedure.

2.4.3. CPT Establishment for Multiple-Parent Nodes. Suppose a node N with n states (S_1, S_2, ..., S_n) has k ($k \geq 2$) parents M_1, M_2, ..., M_k, and the node M_j has m_j states, namely, $S_{M_j 1}, S_{M_j 2}, \ldots, S_{M_j m_j}$ ($j = 1, 2, \ldots, k$); the probability of each state of N on the combination of the states of its parent nodes can be denoted by

$$\begin{aligned} &P\left(N = S_{Ni} \,\middle|\, M_1 = S_{M_1 P_1}, M_1 = S_{M_2 P_2}, \ldots, M_1 = S_{M_k P_k}\right), \\ &\quad i = 1, 2, \ldots, n;\ p_j = 1, 2, \ldots, m_j;\ j = 1, 2, \ldots, k. \end{aligned} \tag{12}$$

As we can see, there are a large number of state combinations of its parent nodes, and it is difficult for experts to directly estimate the above probabilities under such situations. Hence, a decomposition method is adopted here to reduce the elicitation workload by simplifying CPT elicitation [49, 50]. For example, when a node A has three parents B, C, and D, its conditional probability on B, C, and D can be approximated by

$$P(A \mid B, C, D) = \alpha P(A \mid B) P(A \mid C) P(A \mid D), \tag{13}$$

where α is a normalization factor to ensure that $\sum_{a \in A} P(a \mid B, C, D) = 1$.

Thus, (12) can be computed as follows:

$$\begin{aligned} &P\left(N = S_{Ni} \,\middle|\, M_1 = S_{M_1 P_1}, M_1 = S_{M_2 P_2}, \ldots, M_1 = S_{M_k P_k}\right) \\ &\quad = \alpha \prod_{j=1}^{k} P\left(N = S_{Ni} \,\middle|\, M_j = S_{M_j P_j}\right), \\ &\quad i = 1, 2, \ldots, n;\ p_j = 1, 2 \ldots, m_j;\ j = 1, 2, \ldots, k, \end{aligned} \tag{14}$$

where α is a normalizing constant to ensure that

$$\sum_{i=1}^{n} P\left(N = S_{Ni} \,\middle|\, M_1 = S_{M_1 P_1}, M_1 = S_{M_2 P_2}, \ldots, M_1 = S_{M_k P_k}\right) = 1. \tag{15}$$

Through the above technique, we can see that the problem of CPT calculation for a node with multiple-parent nodes is transformed to compute the CPTs for a single-parent node. Additionally, estimating $p(N = S_{Ni} \mid M_j = S_{M_j P_j})$ individually will be much easier than directly estimating $P(N = S_{Ni} \mid M_1 = S_{M_1 P_1}, M_1 = S_{M_2 P_2}, \ldots, M_1 = S_{M_k P_k})$.

Table 2: The construction of pairwise comparison matrix.

M in the state of S_{Mj}	S_{N1}	S_{N2}	...	S_{Nn}	w_{ij}
S_{N1}	a_{11}	a_{12}	...	a_{1n}	w_{1j}
S_{N2}	a_{21}	a_{22}	...	a_{2n}	w_{2j}
...	...	...	...	...	...
S_{Nn}	a_{n1}	a_{n2}	...	a_{nn}	w_{nj}
$\lambda_{\max}$		CI =		CR =	

2.5. FBN-Based Risk Analysis

2.5.1. Risk Reasoning Analysis. After obtaining the prior probabilities and CPTs of FBN, combined with the established FBN model, the forward reasoning for prediction of foundation pit collapse risk prior to construction and during construction can be realized by (16). This approach can predict the potential risk of top event T and provide decision-making support for foundation pit construction.

$$\begin{aligned} P(T=t) = &\sum_{1}^{q_1,\ldots,q_n,r_1,\ldots,r_n} P\left(T=t \mid X_1=x_1,\ldots,X_n=x_n,Y_1=y_1,\ldots,Y_m=y_m\right) \\ &\times P\left(X_1=x_1,\ldots,X_n=x_n,Y_1=y_1,\ldots,Y_m=y_m\right) \\ t=&\left\{t_1,t_2,\ldots,t_p\right\};\ x_i=\left\{x_i^1,x_i^2,\ldots,x_i^{q_i}\right\};\ y_j=\left\{y_j^1,y_j^2,\ldots,y_j^{r_j}\right\};\quad i=1,2,\ldots,n;\ j=1,2,\ldots,m, \end{aligned} \tag{16}$$

where $t=\{t_1, t_2, \ldots, t_P\}$ is states range for the leaf node T, $x_i=\{x_i^1, x_i^2, \ldots, x_i^{q_i}\}$ is states range for the root node X_i, and $y_j=\{y_j^1, y_j^2, \ldots, y_j^{r_j}\}$ is states range for the intermediate node Y_i. $P(T=t \mid X_1=x_1, \ldots, X_n=x_n, Y_1=y_1, \ldots, Y_m=y_m)$ represents the CPT of T, and $P(X_1=x_j, X_2=x_j, \ldots, X_n=x_j, Y_1=y_1, \ldots, Y_m=y_m)$ stands for the JPD of the root nodes.

2.5.2. Sensitivity Analysis. In engineering practice, decision makers usually pay more attention to which factors play an important role in foundation pit collapse. In addition, the critical checkpoints are usually determined based on expert knowledge and practical experience. Sensitivity analysis provides an alternative method that observes the relevant changes in the probability distribution of the top event by changing the probability distribution of each factor. The sensitivity performance measure (SPM) proposed by Zhang et al. [37] is applied for sensitivity analysis in this paper and can be calculated by (17). The higher the SPM (X_i) of root node x_i is, the greater the contribution x_i is for the risk sensitivity of top event T.

$$\mathrm{SPM}\left(X_i\right)=\frac{1}{q_i}\sum_{1}^{q_i}\left|\frac{P\left(T=t \mid X_i=x_i\right)-P(T=t)}{P(T=t)}\right|, \tag{17}$$

where t and x_i refer to the state of the top event T and risk factor X_i, respectively.

3. Case Study

3.1. Background. The foundation pit construction in Qianhu Avenue Station in Nanchang Metro Line 2 is chosen as a case study to illustrate a specific application of the proposed approach. The Qianhu Avenue Station is located at the intersection of Qianhu Avenue and Fenghe South Avenue, Honggutan New District, Nanchang City, Jiangxi Province, China. The length of the metro station is 223 m beginning from YCK27 + 254.700 m to YCK27 + 477.700 m. The width of the main structure of the standard section and the end well of the metro station are 20.2 m and 24.2 m, respectively. On the east side of the station, there is a temporary construction site and a vacant greening land, and on the west side of the station, there is Nanchang Hangkong University (shown in Figure 5). In addition, there are four sewage pipelines with a diameter of 800 mm on both sides of the road, only 20 m to the edge of the foundation pit. According to the investigation report, the main strata of the site comprise miscellaneous fill (1-2), silty clay (2-1), medium-coarse sand (2-4-5), round gravel (2-7), and medium weathered argillaceous siltstone (5-1-2), as shown in Figure 6. The groundwater in the station includes perched pore water and bedrock fissure water, and there is no confined water.

Figure 7 shows the working site of the Qianhu Avenue Station construction. The excavation depth of foundation pit is 16 m, and an open-cut method was used in the station construction as shown in Figure 7(a). The retaining structure of the foundation pit consists of diaphragm walls and three rows of inner supports (Figure 7(b)). The three rows of supports are used to restrain the diaphragm wall deflection. The first row of support was concrete support (800 mm × 1000 mm) and the second and third rows of supports were steel supports (Φ609 mm). In addition, the excavation principle of "layering, blocking, symmetry, and balance" is adopted during the foundation pit excavation, as can be seen in Figure 6.

3.2. Risk Identification and Fault Tree Construction. The metro construction accident data from 2004 to 2017 in China were collected through the network, accident investigation reports, and a literature review [51] and analyzed by statistical methods. We found that foundation pit collapse is the main type of accident, accounting for 44% of the total number of accidents. Moreover, foundation pit collapse is considered a large potential risk to personnel safety and surrounding facilities. Therefore, foundation pit collapse risk is chosen as the top event (T) in the FT for the present study.

Due to complexities and uncertainties of the foundation pit construction process, the foundation pit collapse may be

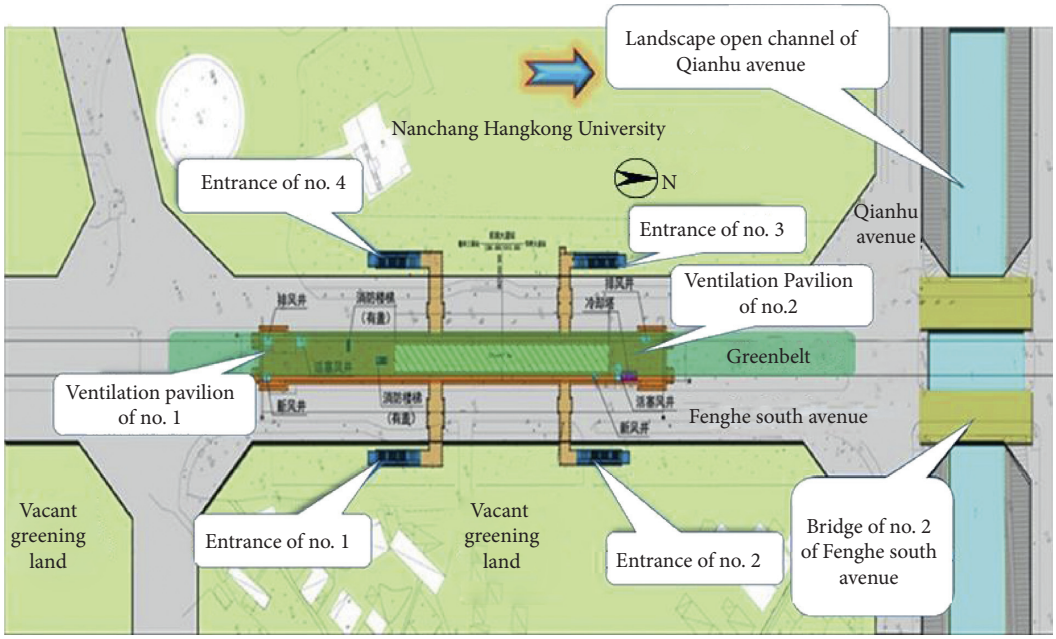

Figure 5: Location relationships of surrounding environment of the metro station.

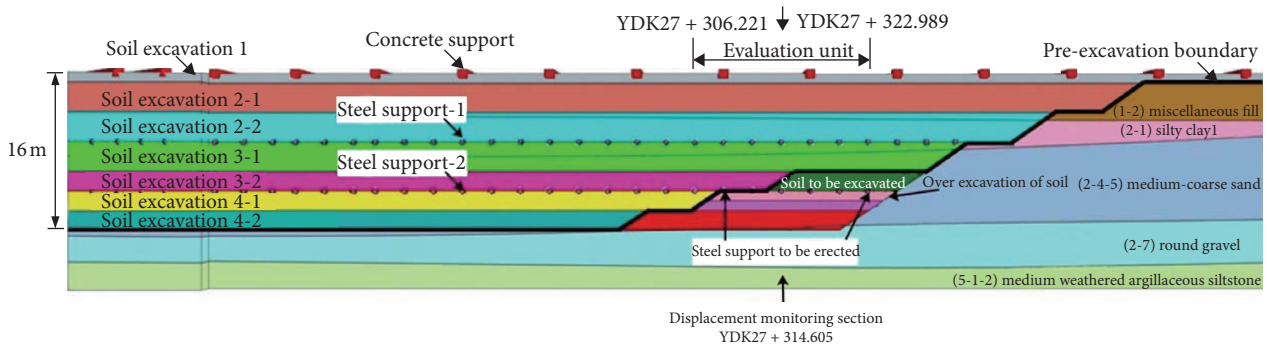

Figure 6: The site geological conditions of the station.

Figure 7: Working site of the Qianhu Avenue Station construction: (a) earth excavation; (b) retaining structure.

influenced by a large number of risk factors that interact with each other. Therefore, a database of 48 deep foundation pit collapse cases of metro stations is analyzed to provide support for risk identification. Moreover, the results of expert inquiry and the method of FT are also used to determine the risk factors and reveal the causal relationships of risk factors. Finally, a FT diagram of foundation pit collapse for the Qianhu Avenue Station is constructed based on the above analysis. The three types of influential factors that contribute to T are revealed and analyzed in detail as follows:

(1) Hydrogeological conditions (y_1): The geological condition (y_4) and hydrologic condition (y_5) are intrinsic risk surroundings; thus, five primary influential factors are selected, namely, thickness of soft stratum or permeable sand layer (x_1), accuracy/degree of site investigation (x_2), groundwater level (x_3), rainfall (x_4), and drainage timeliness (x_5) on the basis of foundation pit collapse case analyses, as shown in Table 3.

(2) Design factors (y_2): The diaphragm walls are widely used in metro foundation pits due to their

Table 3: Node descriptions and risk states division.

Nodes	Descriptions	Risk level/states		
		L (low)	M (medium)	H (high)
T	Foundation pit collapse risk	Slight <22 mm	Moderate 22–30 mm	Serious >30 mm
y_1	Hydrogeological factors	Good 80–100	Moderate 60–80	Poor 0–60
y_2	Design factors	Good 80–100	Moderate 60–80	Poor 0–60
y_3	Construction and management factors	Good 0–100	Moderate 60–80	Poor 0–60
y_4	Geological condition	Good 80–100	Moderate 60–80	Poor 0–60
y_5	Hydrologic condition	Good 80–100	Moderate 60–80	Poor 0–60
y_6	Rationality of diaphragm wall design	Reasonable 80–100	General 60–80	Unreasonable 0–60
y_7	Rationality of support design	Reasonable 80–100	General 60–80	Unreasonable 0–60
y_8	Reliability of excavation	High 80–100	Medium 60–80	Low 0–60
y_9	Reliability of support	High 80–100	Medium 60–80	Low 0–60
y_{10}	Field monitoring and management	Good 80–100	Moderate 60–80	Poor 0–60
x_1	Thickness of soft stratum or permeable sand layer	<1 m	1-2 m	>2 m
x_2	Accuracy/degree of site investigation	Very detailed 80–100	General 60–80	Rough 0–60
x_3	Groundwater level	>16 m	10–16 m	<10 m
x_4	Rainfall	<20 mm/d	20–50 mm/d	>50 mm/d
x_5	Drainage timeliness	In time 80–100	General 60–80	Delay 0–60
x_6	Diaphragm wall thickness	>1000 mm	800–1000 mm	<800 mm
x_7	Diaphragm wall insertion ratio (H_O/H)	>0.4	0.2–0.4	<0.2
x_8	Number of supports	>5	3–5	<3
x_9	Support form	Concrete	Con + ste	Steel
x_{10}	Overbreak depth	<1.0 m	1.0-2.0 m	>2.0 m
x_{11}	Excavation speed	<2500 m^3/d	2500–3000 m^3/d	>3000 m^3/d
x_{12}	Timeliness of support erection	<8 h	8–24 h	>24 h
x_{13}	Specification of support erection	<15 mm	15–30 mm	>30 mm
x_{14}	Steel support axial force	<640 kN	640–1000 kN	>1000 kN
x_{15}	Overloading (multiples of the allowable value of design)	<1.2	1.2–1.5	>1.5
x_{16}	Construction normalization	80–100	60–80	0–60
x_{17}	Monitoring (frequency (times/24 h))	2	1	0

Note. (1) The evaluation of leaf node T is measured by the diaphragm wall deflection, the evaluation of intermediate nodes (y_1, y_2, ..., y_{10}) is measured using 100-mark system, the evaluation of root nodes (x_1, x_3, x_4, x_6 ..., x_{15}, x_{17}) is measured by practical values in actual projects, and the evaluation of root nodes (x_2, x_5, x_{16}) is also measured using 100-mark system. (2) H_O: the insertion depth of diaphragm wall; H: the excavation depth of the foundation pit.

advantages of time and space saving and safety, and they can be used as waterproof curtains during construction and permanent basement walls after construction. And the inner supports are being indispensable part of the diaphragm walls as foundation pits have become deep and large, because they can effectively restrain the diaphragm wall deflection. Therefore, the rationality of diaphragm wall and support design (y_6 and y_7) has great impact on the stability and safety of the pit. The diaphragm wall thickness (x_6), diaphragm wall insertion ratio (H_O/H) (x_7), number of supports (x_8), and support form (x_9) are selected based on the cases analysis, as shown in Table 3.

(3) Construction and management factors (y_3): The construction quality and management level play a crucial role in the pit stability, and improper construction organization and management may lead to potential risks during pit construction. They can be further classified into three types: reliability of excavation (y_8), reliability of support (y_9), and field monitoring and management (y_{10}). Then, the eight primary risk factors (x_{10}, x_{11}, ..., x_{17}) related to construction and management are selected according to the cases analysis, as shown in Table 3.

3.3. Bayesian Network Modeling. The BN model (shown in Figure 8) for collapse risk analysis of metro pit construction can be established in light of the transformation process described in Section 3.2. Each node of BN and relevant descriptions are shown in Table 3. All the nodes are considered to be multistate variables to make the results more accurate. Thus, the corresponding risk state of each node is divided into three levels defined by "L (low), M (medium), and H (high)," as illustrated in Table 3.

3.4. Prior Probabilities and CPT Establishment. First, detailed information about the project's geological exploration, design, construction, and field investigation should be collected. Then, domain experts are invited to express their opinions towards each node of the FBN. Clemen and Winkler [52] indicated that 3 to 5 experts are enough to achieve the most of the knowledge. Thus, we invited five domain experts to elicit prior probabilities and CPTs of the FBN based on the collected information and their own experiences.

The root node X_4 (rainfall) is taken as an example. The probabilities of X_4 in each state can be elicited from experts through the procedure introduced in Section 2.4.1. Each expert individually gives a pairwise comparison matrix $A^{(k)} = [a_{ij}^{(k)}]_{3\times3}$ in the light of Table 2 and a subjectivity reliability level ψ_k towards all states of the root node X_4, and the fuzzy positive

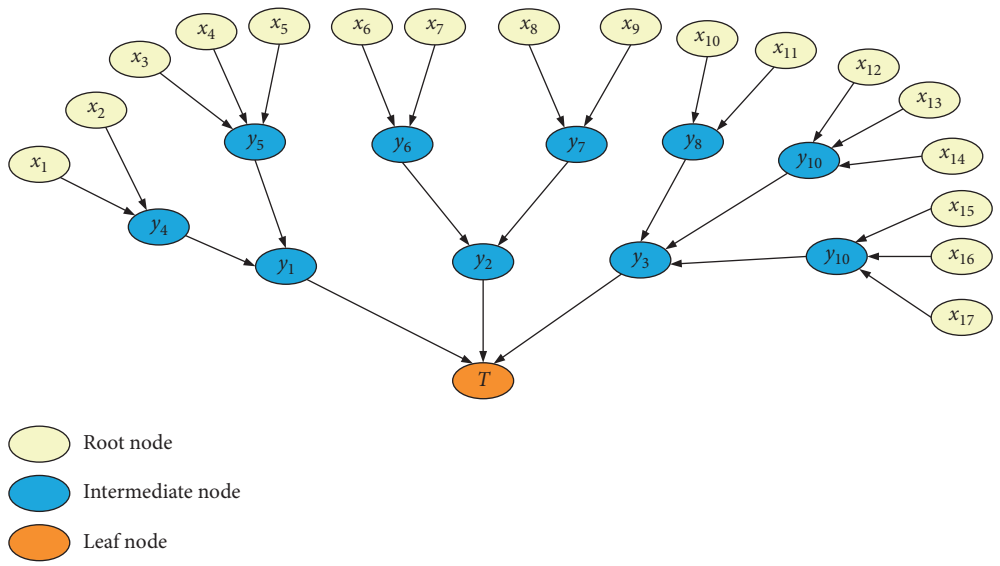

Figure 8: Established BN model for collapse risk analysis of metro foundation pit construction.

reciprocal matrix $\widetilde{A} = [\widetilde{a}_{ij}]_{3\times3}$ shown in Table 4 can be obtained by integrating the five experts' judgements. Then, we can obtain the prior probabilities of node X_4 by calculating the principle eigenvector of the fuzzy matrix $\widetilde{A} = [\widetilde{a}_{ij}]_{3\times3}$ (displayed in Table 4), and these probabilities are shown as follows:

$$\begin{aligned} P(X_4 = L) &= w_L = 0.2631, \\ P(X_4 = M) &= w_M = 0.5851, \\ P(X_4 = H) &= w_H = 0.1518. \end{aligned} \tag{18}$$

The prior probabilities of remaining nodes can also be determined and their prior probabilities are listed in Table 5.

After the prior probabilities of each root node are calculated, CPT elicitation for intermediate nodes and leaf node can be carried out using the FAHP and decomposition method mentioned in Section 3.3.3. The calculation of the CPT of node T is taken as an example. The leaf node T has three parent nodes, as illustrated in the FBN model, namely, y_1, y_2, and y_3. First, we should obtain $P(T|y_1)$, $P(T|y_2)$, and $P(T|y_3)$, respectively, according to the method in Section 2.4.3. An example of the calculation of the probabilities of node T when the node y_1 is at state L is presented in Table 6. Similarly, the probability of each state of T when its parent node y_1 is at states M and H can also be obtained (shown in Table 7). In addition, the probabilities of each state of node T can also be obtained under the given states of nodes y_2 and y_3, and the results are listed in Tables 8 and 9, respectively.

Table 4: The evaluation of prior probabilities of root node X_4.

X_4	L	M	H	ω
L	(1.000, 1.000, 1.0000)	(0.2500, 0.3151, 0.3333)[a]	(0.5000, 0.5000, 0.5000)[a]	$w_L = 0.2631$
M	(3.000, 3.1736, 4.0000)[b]	(1.0000, 1.0000, 1.0000)	(2.000, 2.6723, 3.0000)[a]	$w_M = 0.5851$
H	(2.000, 2.000, 2.0000)[b]	(0.3333, 0.3742, 0.5000)[b]	(1.0000, 1.0000, 1.0000)	$w_H = 0.1518$
CI = 0.0163		CR = 0.0281 < 0.1		$\lambda_{max} = 3.0326$

[a]Experts' judgements after integration. [b]Reciprocal matrix of experts' judgements after integration.

Then, the conditional probabilities of the leaf node T can be estimated via the decomposition method as follows. For instance, when the states of nodes y_1, y_2, and y_3 are all H, we will have the following equations with $\alpha = 1/K$:

$$\begin{aligned} P(T = L \mid y_1 = H, y_2 = H, y_3 = H) &= \alpha P(T = L \mid y_1 = H) P(T = L \mid y_2 = H) P(T = L \mid y_3 = H), \\ P(T = M \mid y_1 = H, y_2 = H, y_3 = H) &= \alpha P(T = M \mid y_1 = H) P(T = M \mid y_2 = H) P(T = M \mid y_3 = H), \\ P(T = H \mid y_1 = H, y_2 = H, y_3 = H) &= \alpha P(T = H \mid y_1 = H) P(T = H \mid y_2 = H) P(T = H \mid y_3 = H), \end{aligned} \tag{19}$$

where

$$\begin{aligned} K = {} & P(T = L \mid y_1 = H) P(T = L \mid y_2 = H) P(T = L \mid y_3 = H) + P(T = M \mid y_1 = H), \\ & P(T = M \mid y_2 = H) P(T = M \mid y_3 = H) + P(T = H \mid y_1 = H) P(T = H \mid y_2 = H) P(T = H \mid y_3 = H). \end{aligned} \tag{20}$$

Table 5: Prior probabilities of each root node.

Root node	L	M	H
X_1	0.2777	0.5814	0.1408
X_2	0.6393	0.2479	0.1128
X_3	0.2067	0.6794	0.1139
X_4	0.2631	0.5851	0.1518
X_5	0.6308	0.2912	0.0780
X_6	0.2844	0.5964	0.1192
X_7	0.2948	0.6242	0.0810
X_8	0.2403	0.6459	0.1138
X_9	0.6183	0.3041	0.0776
X_{10}	0.5311	0.3066	0.1624
X_{11}	0.6627	0.2239	0.1135
X_{12}	0.6412	0.2466	0.1122
X_{13}	0.2864	0.5954	0.1182
X_{14}	0.6552	0.2328	0.1120
X_{15}	0.6723	0.2225	0.1052
X_{16}	0.5828	0.2928	0.1143
X_{17}	0.3455	0.5010	0.1536

Table 6: The evaluation of conditional probabilities of leaf node T on y_1.

$y_1 = L$	L	M	H	ω
L	(1.000, 1.000, 1.0000)	(0.3333, 0.4049, 0.5000)[a]	(0.1667, 0.1810, 0.200)[a]	$w_L = 0.6714$
M	(2.000, 2.4698, 3.000)[b]	(1.000, 1.000, 1.0000)	(0.250, 0.2780, 0.3333)[a]	$w_M = 0.2230$
H	(5.000, 5.5255, 6.0000)[b]	(3.000, 3.5970, 4.0000)[b]	(1.000, 1.000, 1.0000)	$w_H = 0.1056$
CI = 0.0176		CR = 0.0303 < 0.1		$\lambda_{\max} = 3.0352$

[a]Experts' judgements after integration. [b]Reciprocal matrix of experts' judgements after integration.

Table 7: The conditional probabilities of leaf node T on y_1's various states.

T	$y_1 = L$	$y_1 = M$	$y_1 = H$
L	0.7053	0.3102	0.0640
M	0.2371	0.4954	0.2205
H	0.0576	0.1944	0.7155

Table 8: The conditional probabilities of leaf node T on y_2's various states.

T	$y_2 = L$	$y_2 = M$	$y_2 = H$
L	0.6828	0.2535	0.0763
M	0.2490	0.5062	0.1915
H	0.0682	0.2403	0.7322

Table 9: The conditional probabilities of leaf node T on y_3's various states.

T	$y_3 = L$	$y_3 = M$	$y_3 = H$
L	0.7018	0.2079	0.0809
M	0.2395	0.5262	0.1345
H	0.0587	0.2659	0.7846

The following results can be obtained based on the partial probability data in Tables 7–9 along with the above equations:

$$\begin{aligned} P\left(T = L \mid y_1 = H, y_2 = H, y_3 = H\right) &= 0.0008, \\ P\left(T = M \mid y_1 = H, y_2 = H, y_3 = H\right) &= 0.0313, \\ P\left(T = H \mid y_1 = H, y_2 = H, y_3 = H\right) &= 0.9679. \end{aligned} \tag{21}$$

In the same way, we can also obtain the conditional probabilities of T on the other states combination of its parent nodes (y_1, y_2, and y_3). In addition, the CPTs of each intermediate node of BN can be generated similarly. Owing to limited space, only the fuzzy CPT of T is given, as shown in Table 10.

3.5. FBN-Based Risk Analysis

3.5.1. Risk Prediction Based on Forward Reasoning. After prior probabilities and CPTs are assigned into the established FBN model, we can predict the risk of foundation pit collapse by forward reasoning prior to foundation pit construction. This can help decision makers gain insight into the potential risks associated with the foundation pit, which is very important for decision making in the preconstruction phase. Using (16), the occurrence probabilities of foundation pit collapse with different risk levels under prior probability environments (Scenario 1 displayed in Table 11) are calculated as follows:

Table 10: Fuzzy CPT of the leaf node T in the FBN.

y_1	y_2	y_3	$P(T=L \mid y_1, y_2, y_3)$	$P(T=M \mid y_1, y_2, y_3)$	$P(T=H \mid y_1, y_2, y_3)$
L	L	L	0.9745	0.0251	0.0004
L	L	M	0.8930	0.1058	0.0012
L	L	H	0.7541	0.2109	0.0350
L	M	L	0.8376	0.1588	0.0036
L	M	M	0.5299	0.4626	0.075
...	...	...	...	...	...
H	M	H	0.0073	0.1275	0.8652
H	H	L	0.0656	0.2430	0.6913
H	H	M	0.0189	0.3221	0.6590
H	H	H	0.0080	0.0313	0.9679

Table 11: Probabilities of foundation pit collapse under different scenarios.

Scenarios	Evidence	L	M	H	Risk level
Scenarios 1	No	0.47	0.45	0.08	L
Scenarios 2	$P(X_{10}, X_{11}, X_{12}, X_{15}=M)=1$	0.34	0.52	0.14	M

$$
\begin{aligned}
P(T=L) &= \sum_{x_1,\ldots,x_{17},y_1,\ldots,y_{10}} P\left(T=L \mid x_1, x_2, \ldots, x_{17}, y_1, y_2, \ldots, y_{10}\right) \\
&\quad \times P\left(x_1, x_2, \ldots, x_{17}, y_1, y_2, \ldots, y_{10}\right) = 0.47, \\
P(T=M) &= \sum_{x_1,\ldots,x_{17},y_1,\ldots,y_{10}} P\left(T=M \mid x_1, x_2, \ldots, x_{17}, y_1, y_2, \ldots, y_{10}\right) \\
&\quad \times P\left(x_1, x_2, \ldots, x_{17}, y_1, y_2, \ldots, y_{10}\right) = 0.45, \\
P(T=H) &= \sum_{x_1,\ldots,x_{17},y_1,\ldots,y_{10}} P\left(T=H \mid x_1, x_2, \ldots, x_{17}, y_1, y_2, \ldots, y_{10}\right) \\
&\quad \times P\left(x_1, x_2, \ldots, x_{17}, y_1, y_2, \ldots, y_{10}\right) = 0.08.
\end{aligned}
\tag{22}
$$

Obviously, the above computation results mean that the risk state of foundation pit collapse belongs to level L (low) since $P(T=L)>P(T=M)>P(T=H)$. However, the potential risk of foundation pit collapse shows a considerable trend moving towards level M (medium). Thus, the planners and engineers need to optimize the design and construction plans continuously until the collapse risk probability of level M is relatively small to ensure the safety of the foundation pit construction.

Moreover, the actual status information of root nodes will be revealed gradually as the construction progress evolves. Therefore, we can achieve dynamic risk analysis of foundation pit collapse by the new evidence (current actual state of root node) entered into the FBN, which is also the unique merit of the FBN compared to other static analysis methods (FTA, ETA, etc.). When the foundation pit was excavated between YDK27 + 306.221 m and YDK27 + 322.989 m (current evaluation unit shown in Figure 6), there were several irregularities in the current evaluation unit according to the construction plan and on-site inspection. For example, considering the condition of earthwork overbreak, the excavation speed is relatively too fast, the support erection lags, and there are earthmoving vehicles passing along the periphery of the foundation pit. Specifically, the second row of steel support should be set up when the soil is excavated to the level of 11.5 m in light of the design requirements. Actually, the second row of steel support is erected until the soil is excavated to the level of 13 m, as shown in Figure 6 (overbreak part of earthwork). Furthermore, there is overloading around the foundation pit as the earthmoving vehicles pass along the periphery of the foundation pit. Therefore, the new status of root nodes X_{10}, X_{11}, X_{12}, and X_{15} can be defined according to the current construction states as $P(X_{10}, X_{11}, X_{12}, X_{15}=M)=1$ (Scenario 2 displayed in Table 11). Then, we can calculate the occurrence probabilities of foundation pit collapse with different risk levels under current construction status through forward reasoning. Using (16), these probabilities are calculated as follows:

$$
\begin{aligned}
P(T=L) &= \sum_{x_1,\ldots,x_{17},y_1,\ldots,y_{10}} P\left(T=L \mid x_1,\ldots,x_9,x_{10}=x_{11}=x_{12}=x_{15}=M,x_{13},x_{14},x_{16},x_{17},y_1,y_2,\ldots,y_{10}\right) \\
&\quad \times P\left(x_1,x_2,\ldots,x_{17},y_1,y_2,\ldots,y_{10}\right)=0.34, \\
P(T=M) &= \sum_{x_1,\ldots,x_{17},y_1,\ldots,y_{10}} P\left(T=M \mid x_1,\ldots,x_9,x_{10}=x_{11}=x_{12}=x_{15}=M,x_{13},x_{14},x_{16},x_{17},y_1,y_2,\ldots,y_{10}\right) \\
&\quad \times P\left(x_1,x_2,\ldots,x_{17},y_1,y_2,\ldots,y_{10}\right)=0.52, \\
P(T=H) &= \sum_{x_1,\ldots,x_{17},y_1,\ldots,y_{10}} P\left(T=H \mid x_1,\ldots,x_9,x_{10}=x_{11}=x_{12}=x_{15}=M,x_{13},x_{14},x_{16},x_{17},y_1,y_2,\ldots,y_{10}\right) \\
&\quad \times P\left(x_1,x_2,\ldots,x_{17},y_1,y_2,\ldots,y_{10}\right)=0.14.
\end{aligned}
\tag{23}
$$

From the above calculation results, it can be seen that the risk level of foundation pit collapse corresponds to M (medium) as $P(T=M) > P(T=L) > P(T=H)$. In addition, it should be noted that the occurrence probability of risk level H increases from 0.08 to 0.14, meaning that the potential risk of serious collapse is increasing. Hence, necessary measures must be adopted to reduce the occurrence probability of foundation pit collapse risk. Specifically, the earth excavation must be stopped immediately; in the meantime, the steel support should be set up in time. Moreover, the supervisors should strictly control the earth excavation speed and pay much more attention to the overloading condition around the foundation pit while limiting it to a reasonable range.

3.5.2. Comparison with Field Actual Status and Numerical Results. To validate the reliability of the proposed approach, the field monitoring data and numerical simulation results under current construction states (Scenario 2 displayed in Table 11) are analyzed. First, the relationship between collapse risk levels and diaphragm wall deflection is established as illustrated in Table 12 in light of the related design code, the control standards, and the actual construction situation (Nanchang Metro in China). Then, the monitoring data of diaphragm wall deflection under current evaluation unit are analyzed to assess the actual risk status of the foundation pit according to the relationship between collapse risk levels and diaphragm wall deflection shown in Table 12. Actually, the maximum diaphragm wall deflection in the displacement monitoring section of YDK27 + 314.605 was 28.7 mm under current evaluation unit, indicating that the risk level of the foundation pit collapse corresponds to level M. Obviously, the result obtained from the proposed approach was consistent with the field actual status of foundation pit in construction. In addition, early warning was issued on-site since the displacement rate exceeded the warning value (>3 mm/d) for consecutive two days under current construction states.

Moreover, to further illustrate the performance of foundation pit and retaining structure under current construction states, a numerical model of typical construction section under current evaluation unit was established using FLAC3D software [53] and is shown in Figure 9. As Mohr-Coulomb model can predict the retaining structure deformation and ground surface settlement of the foundation pit with reasonable accuracy [54, 55], the Mohr-Coulomb yield criterion was adopted for the rock and soil material. The diaphragm wall and inner supports belong to structural member and were described by elasticity constitutive model. The horizontal constraint is applied on the left and right boundaries of the model, the front and back boundaries are fixed in the Y direction, and the full boundary constraint is applied on the bottom boundary. In addition, an interface element is arranged between the diaphragm wall and the soil layer to simulate the soil-structure interaction such as sliding and opening. The physical and mechanical parameters of material and structure applied in the numerical model are shown in Tables 13 and 14, respectively.

First, the numerical model was calibrated via repeated trial based on the existing monitoring data. On this basis, the horizontal displacements of the diaphragm wall along the depth, considering the condition of earthwork overbreak and overloading around the pit, were calculated adopting the above numerical model. The overbreak depth is 1.5 m, the position of the overloading is at a distance of 5 m from the top of the pit, and the overloading value is 30 kPa. The monitoring and simulating curves of diaphragm wall deflection are shown in Figure 10. It can be seen that the maximum diaphragm wall deflection calculated by FLAC3D is 22.5 mm, and it is also indicated that the risk level of the foundation pit collapse was M according to Table 12. It is apparent that the result obtained from the proposed approach was also in accordance with the numerical result. In addition, the calculation value of maximum diaphragm wall deflection is less than the monitoring value due to only the condition of earthwork overbreak and overloading considered in numerical computation. In other words, the influence of excavation speed, timeliness of support erection, and other uncertainty factors (time-space effect, weather change, etc.) was not considered in numerical calculation. In short, the accuracy and rationality of the proposed approach were verified by comparing with field actual status and numerical results.

3.5.3. Critical Risk Factor Identification and Countermeasures. In construction practice, decision makers usually pay more attention to which factors play a vital role in foundation pit collapse. However, during the process of actual construction, the critical checkpoints are usually determined based on expert knowledge and practical experience. Through sensitivity analysis, the BN can automatically identify the critical

Table 12: Risk level of foundation pit collapse.

Risk level	L (mm)	M (mm)	H (mm)
Diaphragm wall deflection	<22	22–30	>30

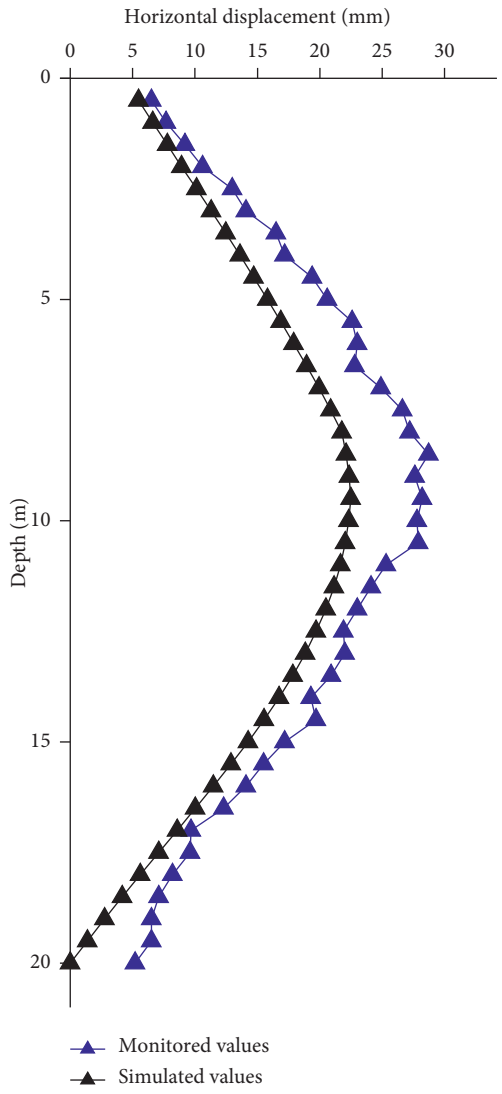

Figure 9: The monitoring and simulating curves of lateral displacements of diaphragm wall.

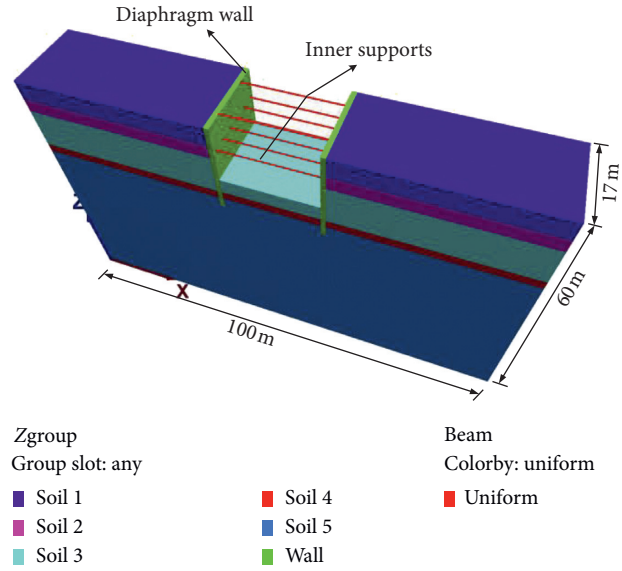

Figure 10: The finite element mesh of the numerical model.

risk factors, and this technique is effective and efficient for controlling the risk of targeted events. The SPM values of all the root nodes (X_i; $i = 1, 2, \ldots, 17$) in Scenario 1 are computed by (17), as shown in Figure 11. When $T = H$, we sort the risk factors according to the SPM value as $X_{11} > X_{12} = X_{16} > X_7 > X_6 > X_9 = X_{10} = X_{14} = X_{15} > X_5 > X_1 = X_4 = X_8 = X_{17} > X_3 > X_{13} > X_2$. It is apparent that X_{11} (excavation speed), X_{12} (timeliness of support erection), and X_{16} (construction normalization) were the top three suspected factors when serious collapse occurred. Therefore, it is essential to give priority to the factors X_{11}, X_{12}, and X_{16} during foundation pit construction. In addition, we can facilitate fault diagnosis according to the following route: $X_{11} \longrightarrow X_{12} \longrightarrow X_{16} \longrightarrow X_7 \longrightarrow X_6 \longrightarrow X_9 \longrightarrow X_{10} \longrightarrow X_{14} \longrightarrow X_{15}$. Furthermore, decision makers can adopt corresponding safety control measures in advance on the basis of the above sensitivity analysis results. For instance, importance should be attached to the restriction of excavation speed during excavation, the inner support should be erected in time, and the management of on-site construction should be strengthened in the meantime.

4. Discussion

Conducting accurate and quantitative risk assessment of foundation pit collapse is difficult or not even possible due to complexities and uncertainties of the foundation pit construction process. Therefore, the conventional methods (FTA, ETA, BN, etc.) cannot usually present the reliable and trustworthy results for us in this case. The proposed risk analysis method is superior to the conventional methods, mainly in the following aspects: firstly, the problems of vagueness and subjectivity are well solved by using a FAHP and improved expert elicitation considering a confidence index; in the meantime, a decomposition method is adopted in this study to reduce the elicitation workload and the possibility of inconsistency by simplifying CPT elicitation; secondly, since the occurrence probability of foundation pit collapse risk can be calculated quantitatively using both the prior probability and the actual fault state revealed during construction of the root nodes, the proposed method can achieve real-time deductive reasoning, dynamic risk control, and management during construction; and finally, the critical risk factors can be identified automatically through

Table 13: The physical and mechanical parameters of model material.

Material	Layer thickness (m)	Deformation modulus (MPa)	Poisson's ratio	Unit Weight (kN/m^3)	Cohesion force (kPa)	Friction angle (°)
Miscellaneous fill	4.4	4	0.30	18.4	4	18.4
Silty clay	3.0	10	0.30	19.1	16	5
Medium-coarse sand	8.9	15	0.26	19.6	1	22
Round gravel	2.2	20	0.24	20.9	1	28
Medium weathered argillaceous siltstone	—	1000	0.18	24	800	32

Table 14: The physical and mechanical parameters of model structure.

Structure	Unit Weight (kN/m^3)	Poisson's ratio	Elastic modulus (MPa)	Section size (mm)
Diaphragm wall	24	0.18	3.0×10^4	Thickness is 800 mm
Concrete support	24	0.18	3.0×10^4	800 mm × 1000 mm
Steel support	78	0.28	2.06×10^5	Φ609 mm

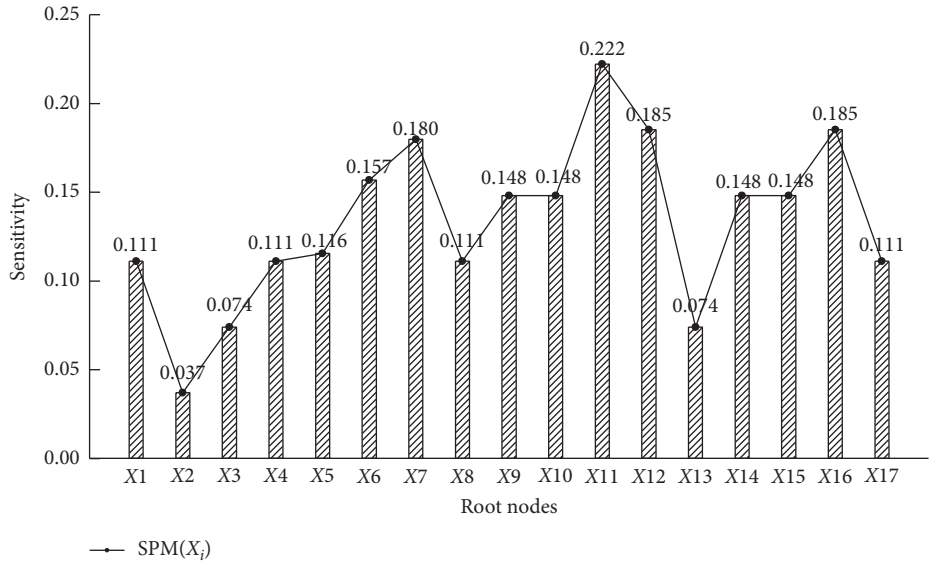

Figure 11: The SPM values of each risk factor when $P\ (T=H)=1$.

sensitivity analysis to help decision makers judge the key checkpoints accurately.

The proposed model was applied before and during construction of the foundation pit in Qianhu Avenue Station, and the design and construction schemes were continuously optimized to reduce the collapse risk during foundation pit construction to a maximum extent. The results were in accordance with the field observations and numerical simulation results, indicating that the model proposed in this paper is of certain feasibility and reliability. The Qianhu Avenue Station construction went smoothly and no collapses occurred throughout foundation pit excavation. In addition, the results of sensitivity analysis indicated that X_{11} (excavation speed), X_{12} (timeliness of support erection), and X_{16} (construction normalization) were the top three risk factors influencing the foundation pit collapse in Qianhu Avenue Station.

Nevertheless, the approach proposed in the present study still has some limitations. For example, this approach relies greatly on domain experts during the establishment of prior probabilities and CPTs of the FBN. Although the subjective bias and uncertainty are reduced to some extent by using the FAHP and improved expert elicitation, some subjective bias still remains. Moreover, the risk factors considered in this study are determined based on the results of statistical analysis of foundation pit collapse cases, expert inquiry, and fault tree analysis. Thus, some other risk factors may not be taken into consideration due to the shortage of foundation pit cases. Future work will focus on developing a data-driven BN model by collecting a large number of

foundation pit cases along with field monitoring data to further reduce subjectivity and enhance the robustness of the proposed model.

5. Conclusions

Foundation pit construction is associated with large potential risks owing to various risk events in a complicated uncertain environment. As foundation pit collapse in metro construction can cause heavy casualties and financial losses, it has aroused the attention of all parties. However, uncertain construction environments and data shortages make it difficult to accurately predict the potential collapse risk in foundation pit construction. This study proposes a systematic model for dynamic risk analysis of foundation pit collapse during construction based on a FBN and a FAHP. In terms of priori probabilities and CPTs establishment, a FAHP and decomposition method were adopted to reduce subjectivity and vagueness. In addition, improved expert elicitation considering a confidence index was used to guarantee survey data reliability. A case study concerning an actual deep foundation pit in a metro station was utilized to illustrate a specific application of this model, and the result was in accordance with the field observations and numerical simulation results.

Through the FBN-based risk analysis, the potential risks of foundation pit collapse were predicted quantitatively to help decision makers adopt necessary safety measures in advance; additionally, the critical risk factors were determined automatically to contribute to judging the key checkpoints accurately and effectively. The proposed approach can provide effective decision-making support for planners and engineers and guarantee on-site construction safety of foundation pit. Meanwhile, the results of this study can be used in the field case with similar retaining structure of foundation pit.

Data Availability

The data used to support the findings of this study are included within the article.

Conflicts of Interest

The authors wish to confirm that there are no known conflicts of interest associated with this publication.

Acknowledgments

This work was supported by the National Key R&D Program of China (2017YFC1501304) and China National Natural Science Foundation (51579235 and 41672314).

References

[1] C. C. Zhang and J. M. Li, "Accident analysis for "08.11.15" foundation pit collapse of Xianghu station of Hangzhou metro," *Journal of Geotechnical Engineering*, vol. 2, no. 1, pp. 338–342, 2010, in Chinese.

[2] C. Yang and Z. Zhang, "Safety accident analysis for second phase projects of shenzhen metro," *Railway Engineering*, vol. 1, 2013.

[3] Y. Bai, Z. Dai, and W. Zhu, "Multiphase risk-management method and its application in tunnel engineering," *Natural Hazards Review*, vol. 15, no. 2, pp. 140–149, 2014.

[4] P. Baraldi and E. Zio, "A combined monte carlo and possibilistic approach to uncertainty propagation in event tree analysis," *Risk Analysis*, vol. 28, no. 5, pp. 1309–1326, 2008.

[5] K. You, Y. Park, and J. S. Lee, "Risk analysis for determination of a tunnel support pattern," *Tunnelling and Underground Space Technology*, vol. 20, no. 5, pp. 479–486, 2005.

[6] E.-S. Hong, I.-M. Lee, H.-S. Shin, S.-W. Nam, and J.-S. Kong, "Quantitative risk evaluation based on event tree analysis technique: application to the design of shield TBM," *Tunnelling and Underground Space Technology*, vol. 24, no. 3, pp. 269–277, 2009.

[7] J. Sejnoha, D. Jarušková, O. Spackova, and E. Novotná, "Risk quantification for tunnel excavation process," *World Academy of Science, Engineering and Technology*, vol. 58, pp. 393–401, 2009.

[8] K.-C. Hyun, S. Min, H. Choi, J. Park, and I.-M. Lee, "Risk analysis using fault-tree analysis (FTA) and analytic hierarchy process (AHP) applicable to shield TBM tunnels," *Tunnelling and Underground Space Technology*, vol. 49, pp. 121–129, 2015.

[9] H. B. Zhou, H. Yao, and J. H. Lu, "Construction risk assessment on deep foundation pits of a metro line in Shanghai," *Chinese Journal of Geotechnical Engineering*, vol. 28, no. Supp 1, pp. 1902–1906, 2006, in Chinese.

[10] L. Joshua and K. Varghese, "Selection of accelerometer location on Bricklayers using decision trees," *Computer-Aided Civil and Infrastructure Engineering*, vol. 28, no. 5, pp. 372–388, 2013.

[11] W. Yan, L. Baoguo, and Q. Yi, "Fuzzy analytic network process and its application in tunnel engineering risk analysis," *Electronic Journal of Geotechnical Engineering*, vol. 20, pp. 6685–6701, 2015.

[12] H. Subramanyan, P. H. Sawant, and V. Bhatt, "Construction project risk assessment: development of model based on investigation of opinion of construction project experts from India," *Journal of Construction Engineering and Management*, vol. 138, no. 3, pp. 409–421, 2012.

[13] M. An, Y. Chen, and C. J. Baker, "A fuzzy reasoning and fuzzy-analytical hierarchy process based approach to the process of railway risk information: a railway risk management system," *Information Sciences*, vol. 181, no. 18, pp. 3946–3966, 2011.

[14] A. Nieto-Morote and F. Ruz-Vila, "A fuzzy approach to construction project risk assessment," *International Journal of Project Management*, vol. 29, no. 2, pp. 220–231, 2011.

[15] M. Aboushady, M. Marzouk, and M. G. Elbarkouky, "Fuzzy consensus qualitative risk analysis framework for building construction projects," *International Journal of Architecture, Engineering and Construction*, vol. 3, no. 3, pp. 1160–1165, 2014.

[16] F. Nasirzadeh, A. Afshar, and M. Khanzadi, "Dynamic risk analysis in construction projects," *Canadian Journal of Civil Engineering*, vol. 35, no. 8, pp. 820–831, 2008.

[17] A. Salah and O. Moselhi, "Risk identification and assessment for EPCM projects using fuzzy set theory," *Canadian Journal of Civil Engineering*, vol. 43, no. 5, pp. 429–442, 2016.

[18] H. Nezarat, F. Sereshki, and M. Ataei, "Ranking of geological risks in mechanized tunneling by using Fuzzy Analytical

Hierarchy Process (FAHP)," *Tunnelling and Underground Space Technology*, vol. 50, pp. 358–364, 2015.

[19] A. Mottahedi and M. Ataei, "Fuzzy fault tree analysis for coal burst occurrence probability in underground coal mining," *Tunnelling and Underground Space Technology*, vol. 83, 2019.

[20] G.-H. Zhang, Y.-Y. Jiao, L.-B. Chen, H. Wang, and S.-C. Li, "Analytical model for assessing collapse risk during mountain tunnel construction," *Canadian Geotechnical Journal*, vol. 53, no. 2, pp. 326–342, 2016.

[21] L. A. Zadeh, "Fuzzy sets," *Information and Control*, vol. 8, no. 3, pp. 338–353, 1965.

[22] J. Ren, I. Jenkinson, J. Wang, D. L. Xu, and J. B. Yang, "An offshore risk analysis method using fuzzy Bayesian network," *Journal of Offshore Mechanics & Arctic Engineering*, vol. 131, Article ID 041101, 2009.

[23] E. Zarei, N. Khakzad, V. Cozzani, and G. Reniers, "Safety analysis of process systems using fuzzy Bayesian network (FBN)," *Journal of Loss Prevention in the Process Industries*, vol. 57, pp. 7–16, 2019.

[24] X. Wu, Z. Jiang, L. Zhang, M. J. Skibniewski, and J. Zhong, "Dynamic risk analysis for adjacent buildings in tunneling environments: a Bayesian network based approach," *Stochastic Environmental Research and Risk Assessment*, vol. 29, no. 5, pp. 1447–1461, 2015.

[25] L. Zhang, X. Wu, M. J. Skibniewski, J. Zhong, and Y. Lu, "Bayesian-network-based safety risk analysis in construction projects," *Reliability Engineering & System Safety*, vol. 131, pp. 29–39, 2014.

[26] P.-C. Li, G.-H. Chen, L.-C. Dai, and L. Zhang, "A fuzzy Bayesian network approach to improve the quantification of organizational influences in HRA frameworks," *Safety Science*, vol. 50, no. 7, pp. 1569–1583, 2012.

[27] A. Bobbio, L. Portinale, M. Minichino, and E. Ciancamerla, "Improving the analysis of dependable systems by mapping fault trees into Bayesian networks," *Reliability Engineering & System Safety*, vol. 71, no. 3, pp. 249–260, 2001.

[28] N. Khakzad, F. Khan, and P. Amyotte, "Safety analysis in process facilities: comparison of fault tree and Bayesian network approaches," *Reliability Engineering & System Safety*, vol. 96, no. 8, pp. 925–932, 2011.

[29] R. L. Sousa and H. H. Einstein, "Risk analysis during tunnel construction using Bayesian networks: porto metro case study," *Tunnelling and Underground Space Technology*, vol. 27, no. 1, pp. 86–100, 2012.

[30] W.-J. Liang, D.-F. Zhuang, D. Jiang, J.-J. Pan, and H.-Y. Ren, "Assessment of debris flow hazards using a Bayesian network," *Geomorphology*, vol. 171-172, pp. 94–100, 2012.

[31] N. Khakzad, F. Khan, and P. Amyotte, "Quantitative risk analysis of offshore drilling operations: a Bayesian approach," *Safety Science*, vol. 57, pp. 108–117, 2013.

[32] Y. Zhou, C. Li, C. Zhou, and H. Luo, "Using Bayesian network for safety risk analysis of diaphragm wall deflection based on field data," *Reliability Engineering & System Safety*, vol. 180, pp. 152–167, 2018.

[33] E. J. M. Lauría and P. J. Duchessi, "A Bayesian Belief Network for IT implementation decision support," *Decision Support Systems*, vol. 42, no. 3, pp. 1573–1588, 2006.

[34] A. Mentes and I. H. Helvacioglu, "An application of fuzzy fault tree analysis for spread mooring systems," *Ocean Engineering*, vol. 38, no. 2-3, pp. 285–294, 2011.

[35] N. Xia, P. X. W. Zou, X. Liu, X. Wang, and R. Zhu, "A hybrid BN-HFACS model for predicting safety performance in construction projects," *Safety Science*, vol. 101, pp. 332–343, 2018.

[36] M. Hanss, "On the implementation of fuzzy arithmetical operations for engineering problems," in *Proceedings of the 18th International Conference of the North American Fuzzy Information Processing Society*, pp. 462–466, New York, NY, USA, June 1999.

[37] L. Zhang, X. Wu, Y. Qin, M. J. Skibniewski, and W. Liu, "Towards a fuzzy Bayesian network based approach for safety risk analysis of tunnel-induced pipeline damage," *Risk Analysis*, vol. 36, no. 2, pp. 278–301, 2015.

[38] Z. Z. Wang and C. Chen, "Fuzzy comprehensive Bayesian network-based safety risk assessment for metro construction projects," *Tunnelling and Underground Space Technology*, vol. 70, pp. 330–342, 2017.

[39] J. Sun, B. Liu, Z. Chu, L. Chen, and X. Li, "Tunnel collapse risk assessment based on multistate fuzzy Bayesian networks," *Quality & Reliability Engineering International*, vol. 34, no. 8, pp. 1646–1662, 2018.

[40] G. Kabir, R. Sadiq, and S. Tesfamariam, "A fuzzy Bayesian belief network for safety assessment of oil and gas pipelines," *Structure and Infrastructure Engineering*, vol. 12, no. 8, pp. 874–889, 2015.

[41] F. Wang, L. Y. Ding, H. B. Luo, and P. E. D. Love, "Probabilistic risk assessment of tunneling-induced damage to existing properties," *Expert Systems with Applications*, vol. 41, no. 4, pp. 951–961, 2014.

[42] G. Zhang and V. V. Thai, "Expert elicitation and Bayesian network modeling for shipping accidents: a literature review," *Safety Science*, vol. 87, pp. 53–62, 2016.

[43] J. Schäfer and K. Strimmer, "A shrinkage approach to large-scale covariance matrix estimation and implications for functional genomics," *Statistical Applications in Genetics and Molecular Biology*, vol. 4, no. 1, 2005.

[44] I. Tsamardinos, L. E. Brown, and C. F. Aliferis, "The max-min hill-climbing Bayesian network structure learning algorithm," *Machine Learning*, vol. 65, no. 1, pp. 31–78, 2006.

[45] K.-S. Chin, D.-W. Tang, J.-B. Yang, S. Y. Wong, and H. Wang, "Assessing new product development project risk by Bayesian network with a systematic probability generation methodology," *Expert Systems with Applications*, vol. 36, no. 6, pp. 9879–9890, 2009.

[46] T. L. Saaty, *The Analytic Hierarchy Process*, McGraw-Hill, New York, NY, USA, 1980.

[47] J. J. Buckley, "Fuzzy hierarchical analysis," *Fuzzy Sets and Systems*, vol. 17, no. 3, pp. 233–247, 1985.

[48] M. Detyniecki and R. R. Yager, "Ranking fuzzy numbers using α-WEIGHTED valuations," *International Journal of Uncertainty, Fuzziness and Knowledge-Based Systems*, vol. 8, no. 5, pp. 573–591, 2000.

[49] Y. F. Wang, M. Xie, K. M. Ng, and M. S. Habibullah, "Probability analysis of offshore fire by incorporating human and organizational factor," *Ocean Engineering*, vol. 38, no. 17-18, pp. 2042–2055, 2011.

[50] P. Ping, K. Wang, D. Kong, and G. Chen, "Estimating probability of success of escape, evacuation, and rescue (EER) on the offshore platform by integrating Bayesian network and fuzzy AHP," *Journal of Loss Prevention in the Process Industries*, vol. 54, pp. 57–68, 2018.

[51] Q. Qian and P. Lin, "Safety risk management of underground engineering in China: progress, challenges and strategies," *Journal of Rock Mechanics and Geotechnical Engineering*, vol. 8, no. 4, pp. 423–442, 2016.

[52] R. T. Clemen and R. L. Winkler, "Combining probability distributions from experts in risk analysis," *Risk Analysis*, vol. 19, no. 2, pp. 187–203, 1999.

[53] Itasca Consulting Group Inc., *User Manual for FLAC3D, Version.5.0*, Itasca Consulting Group Inc., Minneapolis, MN, USA, 2012.

[54] S. Likitlersuang, C. Surarak, D. Wanatowski, E. Oh, and A. Balasubramaniam, "Finite element analysis of a deep excavation: a case study from the Bangkok MRT," *Soils and Foundations*, vol. 53, no. 5, pp. 756–773, 2013.

[55] X. Cui, M. Ye, and Y. Zhuang, "Performance of a foundation pit supported by bored piles and steel struts: a case study," *Soils and Foundations*, vol. 58, no. 4, pp. 1016–1027, 2018.